NEEDLE1 encodes a mitochondria localized ATP-dependent metalloprotease required for thermotolerant maize growth

Qiujie Liu[a], Mary Galli[a], Xue Liu[a], Silvia Federici[a,b], Amy Buck[a,c], Jon Cody[d], Massimo Labra[b], and Andrea Gallavotti[a,e,1]

[a]Waksman Institute of Microbiology, Rutgers University, Piscataway, NJ 08854-8020; [b]Dipartimento di Biotecnologie e Bioscienze, Università di Milano Bicocca, 20126 Milan, Italy; [c]Section of Cell and Developmental Biology, University of California San Diego, La Jolla, CA 92093-0116; [d]Division of Biological Sciences, University of Missouri Columbia, Columbia, MO 65211; and [e]Department of Plant Biology, Rutgers University, New Brunswick, NJ 08901

Edited by Mark Estelle, University of California San Diego, La Jolla, CA, and approved August 20, 2019 (received for review April 25, 2019)

Meristems are highly regulated structures ultimately responsible for the formation of branches, lateral organs, and stems, and thus directly affect plant architecture and crop yield. In meristems, genetic networks, hormones, and signaling molecules are tightly integrated to establish robust systems that can adapt growth to continuous inputs from the environment. Here we characterized *needle1* (*ndl1*), a temperature-sensitive maize mutant that displays severe reproductive defects and strong genetic interactions with known mutants affected in the regulation of the plant hormone auxin. *NDL1* encodes a mitochondria-localized ATP-dependent metalloprotease belonging to the FILAMENTATION TEMPERATURE-SENSITIVE H (FTSH) family. Together with the hyperaccumulation of reactive oxygen species (ROS), *ndl1* inflorescences show upregulation of a plethora of stress-response genes. We provide evidence that these conditions alter endogenous auxin levels and disrupt primordia initiation in meristems. These findings connect meristem redox status and auxin in the control of maize growth.

maize | meristems | FTSH | ROS | auxin

Plant developmental plasticity depends on the maintenance of various groups of stem cells called meristems. In particular, shoot architecture in higher plants is established by apical meristems, such as shoot apical meristems (SAMs) and inflorescence meristems (IMs), and axillary meristems (AMs), initiating at the axils of true or modified leaves. In crop species such as maize, IM and AM activity determines inflorescence architecture, thus directly impacting reproductive potential and yield.

Several plant hormones such as auxin and cytokinin, as well as environmental factors, influence meristem function, which entails initiating lateral primordia at the peripheral zone (PZ) while maintaining a stem cell core in the central zone (CZ) of the meristem (1). While cytokinins are necessary for meristem maintenance, auxins are required for primordia initiation, and the action of both is key to meristem activity (2). Recently, the redox status of the SAM, and in particular the balance between superoxide (O_2^-) and hydrogen peroxide (H_2O_2) in the CZ and PZ, have been proposed to integrate stress signals with core meristematic functions (3). These findings complement previous studies whereby mutants affected in meristem redox status show developmental defects (4–9). Understanding how meristem redox regulation is integrated into both transcriptional and hormonal networks is crucial for comprehending plant stress adaptation (10, 11).

Auxins play many roles in plant development. Local auxin concentration gradients are necessary for organ formation, and the dynamic regulation of auxin transport establishes the patterning of inflorescences and reproductive structures (2). In maize, mutants defective in AM initiation and development show a reduction in inflorescence branching and spikelet formation (grass-specific structures containing florets), and often are caused by mutations in auxin-related genes. For example, *SPARSE INFLORESCENCE1* (*SPI1*) encodes a maize ortholog of *Arabidopsis* YUCCAs, enzymes that function in the main auxin biosynthetic pathway in plants (12, 13), and *BARREN INFLORESCENCE1* and *4* (*BIF1* and *BIF4*) encode AUX/IAAs, negative regulators of auxin signaling (14). Here we show that *NDL1* encodes a mitochondrial-localized m-AAA protease of the FTSH family (15), and that *ndl1* mutants condition high ROS levels that affect auxin homeostasis and consequently reproductive organogenesis.

Results

***needle1* Is a Temperature-Sensitive Mutant Affected in Reproductive Organogenesis.** A single allele of the *ndl1* mutant (*ndl1-ref*) was originally identified in an EMS mutagenesis screen for maize inflorescence mutants. Segregation in M2 populations indicated that the phenotype was caused by a single recessive mutation. After introgression into a homogeneous B73 background, homozygous *ndl1* plants showed a range of inflorescence phenotypes, with the strongest defects observed in the tassel, where phenotypes ranged from tassels with a slightly reduced number of branches and spikelets to those with no branches and spikelets on the main spike; ears of *ndl1* plants were marginally shorter than wild type and occasionally showed disorganized rows of kernels (Fig. 1 *A–D* and *SI Appendix*, Fig. S1).

Significance

Meristems are highly regulated groups of stem cells that are ultimately responsible for the formation of all branches, lateral organs, and stems in plants, and thus directly affect plant architecture and crop yield. We have identified a highly conserved member of a family of mitochondria-localized proteases that regulates maize inflorescence architecture. Unlike in *Arabidopsis*, in which its function appears dispensable, we have discovered that this protein is required for maize growth and productivity in field conditions and in high temperatures, and we provide evidence that it maintains reproductive meristem redox status and auxin homeostasis. These data highlight the importance of meristem redox status for sustaining maize organogenesis in challenging environments.

Author contributions: Q.L., M.G., X.L., S.F., and A.G. designed research; Q.L., M.G., X.L., S.F., A.B., J.C., and A.G. performed research; Q.L., M.G., S.F., M.L., and A.G. analyzed data; and Q.L., M.G., and A.G. wrote the paper.

The authors declare no conflict of interest.

This article is a PNAS Direct Submission.

Data deposition: The NDL1 coding sequence was deposited in GenBank, https://www.ncbi.nlm.nih.gov/genbank/ (accession no. MK674049) and corresponds to GRMZM2G038401/Zm00001d010522_T001 (B73 v3/v4). RNA-seq datasets were deposited in the Gene Expression Omnibus (GEO) database, https://www.ncbi.nlm.nih.gov/geo (accession nos. GSE129684 and GSE135468).

[1]To whom correspondence may be addressed. Email: agallavotti@waksman.rutgers.edu.

This article contains supporting information online at www.pnas.org/lookup/suppl/doi:10.1073/pnas.1907071116/-/DCSupplemental.

First published September 9, 2019.

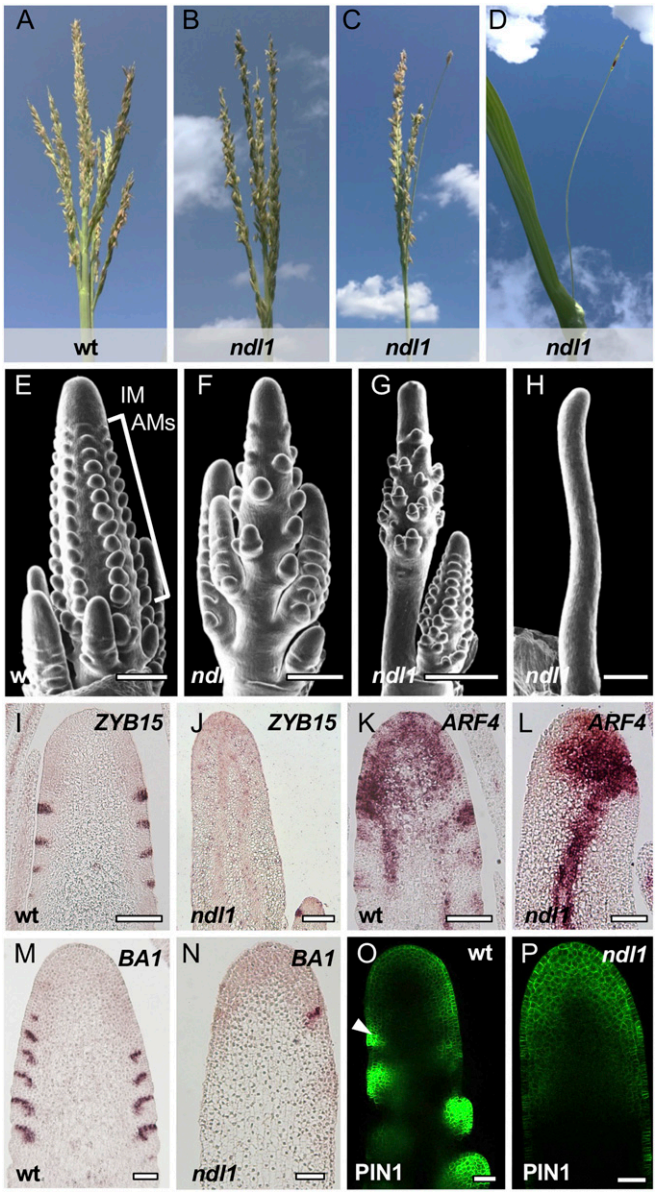

Fig. 1. *ndl1* is defective in reproductive organogenesis. (*A–D*) The *ndl1* tassel phenotype is very variable, from mild (*B*) to severe (*D*). (*E–H*) SEMs of immature tassels in normal and mutant plants also show different expressivity of the *ndl1* mutation. AMs, axillary meristems; IM, inflorescence meristem. (Scale bars, 500 μm.) (*I–N*) mRNA in situ hybridizations of immature tassels with *ZYB15*, *ARF4*, and *BA1* antisense probes. (Scale bars, 250 μm.) (*O* and *P*) Confocal images of normal and *ndl1* immature tassels expressing ZmPIN1a-YFP; arrowhead points to PIN1-YFP up-regulation at the site of primordia initiation. (Scale bars, 100 μm.)

The variable expressivity of the *ndl1* tassel phenotype was observed in both field and greenhouse conditions; however, the appearance of a strong phenotype in field-grown plants was more likely to occur in late planting fields, i.e., June instead of May, with ∼10 °F higher temperatures (*SI Appendix*, Fig. S2). To test the hypothesis that temperature was influencing the expressivity of the *ndl1* phenotype, we grew *ndl1* plants in a growth chamber at mild (24 °C day/20 °C night) and high temperatures (32 °C day/28 °C night). At high temperatures, over 30% of *ndl1* plants arrested growth after producing a few leaves, while the remaining *ndl1* plants transitioned to flowering but produced tassels with significantly fewer branches than wild type plants (*SI Appendix*, Fig. S2). None of these phenotypes were observed at mild temperature. We also determined that *ndl1* mutants displayed significantly shorter primary roots when grown at increasingly higher temperatures than wild type plants grown in the same conditions (*SI Appendix*, Fig. S1). These results indicate that *ndl1-ref* is a temperature-sensitive mutant that shows vegetative and reproductive defects at high temperatures.

To characterize *ndl1* inflorescence defects, we used SEM in the early stages of tassel and ear development. In wild type plants, the IM gives rise to a series of reproductive AMs, which subsequently produce spikelets and florets (Fig. 1*E*). In severe *ndl1* tassels, no AMs were visible, whereas in tassels with a weak phenotype, the regular initiation and arrangements of AMs along the inflorescence axis was partially disrupted (Fig. 1 *F–H*). In *ndl1* ears, we observed milder defects in AM initiation compared with tassels, and IMs occasionally showed slight fasciation (*SI Appendix*, Fig. S1). Altogether, these results suggest that *NDL1* functions in AMs initiation as well as in IM maintenance.

In maize inflorescences, the early steps of primordia initiation occur within the PZ of the IM, where suppressed bracts (SBs), the first visible primordia, subtend newly initiating AMs. We used antisense probes for the maize *ZYB15*, *BA1*, and *ARF4* genes whose expression marks SBs, boundary domains, and meristems, respectively (Fig. 1 *I*, *K*, and *M*), to analyze the early steps of reproductive organogenesis (14, 16). In *ndl1* immature tassels, the regular expression patterns of *ZYB15* and *BA1* were absent in the PZ of the IM (Fig. 1 *I*, *J*, *M*, and *N*). Similarly, *ARF4*, whose expression is typically observed in both the IM and the PZ in wild type (14), was expressed normally in the *ndl1* IM but absent in the PZ (Fig. 1 *K* and *L*).

Polar auxin transport is necessary for maize AM initiation and inflorescence patterning (17, 18), and ZmPIN1a is a membrane-localized auxin efflux transporter whose up-regulation at the PZ of IMs marks newly initiating primordia. We therefore monitored the expression of ZmPIN1a-YFP in wild type and *ndl1* immature tassels. A strong up-regulation of ZmPIN1a-YFP was detected on the flank of wild type IMs, which overlapped with SB and AM initiation sites as previously reported (Fig. 1*O*) (18). This patterning was absent in phenotypically severe *ndl1* tassels (Fig. 1*P*), while, in mild *ndl1* tassels, ZmPIN1a-YFP localization resembled the wild type pattern of expression (*SI Appendix*, Fig. S3). Overall, our results indicate that *NDL1* is essential for the early stages of reproductive organogenesis leading to the initiation of SBs and AMs.

ndl1 inflorescence defects were reminiscent of previously described maize mutants affected in auxin biology (12, 14, 17, 19). This observation together with the disruption of ZmPIN1a-YFP expression in *ndl1* tassels suggested that *NDL1* may affect auxin-related processes. We therefore examined the genetic interaction between *ndl1* and auxin-related mutants defective in signaling and biosynthesis. We observed a strong genetic interaction between *ndl1* and *Bif1*, a semidominant auxin signaling mutant caused by a stabilizing mutation in *ZmIAA27* (14). A similarly strong interaction was seen between *ndl1* and *spi1*, an auxin biosynthetic mutant (12). In both cases, *ndl1* enhanced the inflorescence phenotype of +/*Bif1* and *spi1*/*spi1* mutants (*SI Appendix*, Fig. S4). Double-mutant tassels showed a significant reduction in branch and spikelet-pair number compared with single mutants, while long barren tips in the ears of double mutants were observed (*SI Appendix*, Fig. S4). A similar ear phenotype was also seen when *ndl1* was crossed to semidominant auxin signaling mutant *Bif4* (14) (*SI Appendix*, Fig. S4). Overall, these genetic interactions suggest a functional link between *NDL1* and auxin in regulating maize inflorescence development.

***NDL1* Encodes a Mitochondrial Localized FTSH Protein.** By positional cloning, the *ndl1-ref* allele was mapped to a 1.2-Mb window on chromosome 8, which contained 27 predicted genes (Fig. 2*A*). We then performed bulked segregant RNA-seq analysis (20) and identified an A-to-T transversion that was present only in the *ndl1* mutant within the coding region of *GRMZM2G038401*, a gene encoding a protein homologous to FTSH, a highly conserved

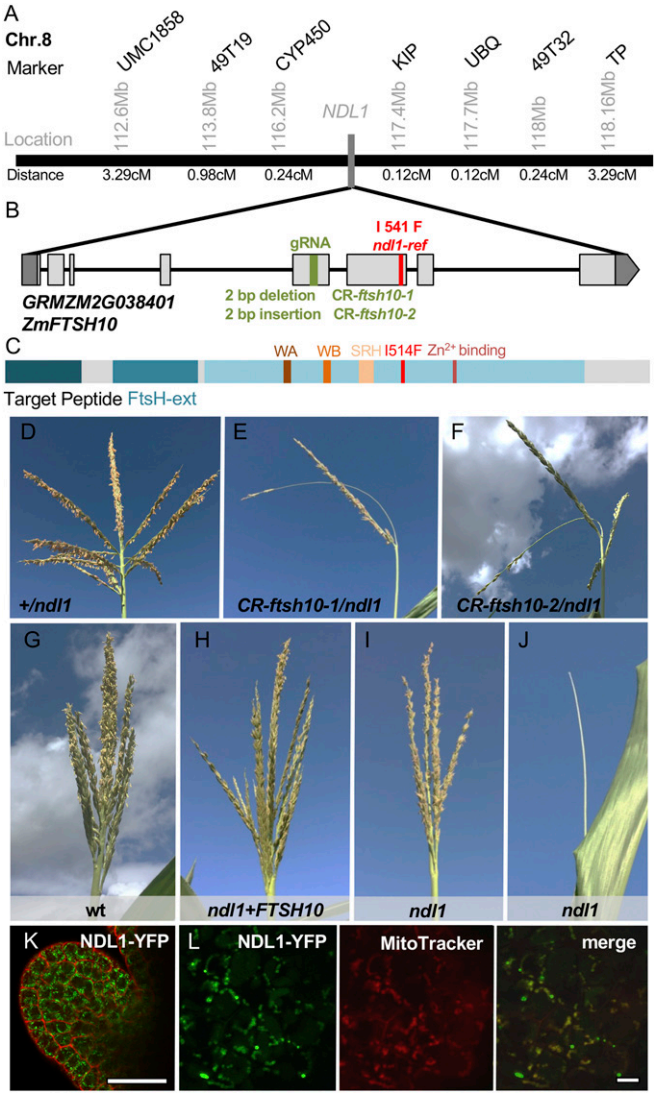

Fig. 2. *NDL1* encodes ZmFTSH10. (*A*) Positional cloning of *NDL1*. Molecular markers used and physical (Mb) and genetic distances (cM) are indicated. (*B*) Schematic representation of the *ZmFTSH10* gene and the position of the mutant alleles. Exons and UTRs are depicted as light gray and dark gray rectangles, respectively. The green bar indicates the guide RNA targeting site. The red bar positions the missense mutation. (*C*) Schematic representation of the ZmFTSH10 protein. FtsH-ext, FtsH-extracellular domain (Pfam); SRH, Second Region of Homology motif; WA, Walker A motif; WB, Walker B motif. (*D–F*) The tassel phenotype of wild type and *ndl1* mutants generated by CRISPR-Cas9. (*G–J*) The variable tassel phenotype of *ndl1* (*I* and *J*) is rescued by the *pZmFTSH10*::*FTSH10-YFP* construct. (*K*) Confocal images of an ear AM expressing FTSH10-YFP, counterstained with propidium iodide. (Scale bar, 50 μm.) (*L*) Confocal images of immature ear AMs expressing NDL1-YFP stained with MitoTracker Red CMXRos. (Scale bars, 10 μm.)

mitochondrial localized protein present in all organisms from bacteria to humans. The resulting amino acid substitution in *ndl1* (I541F) corresponded to a residue that was highly conserved (invariably I or L) in both prokaryotic and eukaryotic organisms (*SI Appendix*, Fig. S5). We then sequenced the candidate gene in 29 inbred lines and examined 900 lines from the maize HapMap 3.1 for SNPs in *GRMZM2G038401* (21) and determined that the A>T SNP was present only in the *ndl1-ref* mutant, suggesting that it was a mutation rather than an extant polymorphism.

We pursued 2 complementary approaches to confirm that *GRMZM2G038401*, hereafter referred to as *ZmFTSH10*, corresponded to *NDL1*. First, we used a CRISPR-Cas9–based strategy with a gRNA targeting exon 5 of *ZmFTSH10* to create additional mutant alleles (Fig. 2*B*). T1 transgenic plants containing the CRISPR-Cas9 vector were crossed to *ndl1-ref* homozygous mutants. A barren tassel phenotype was observed in several individual plants in the resulting F1s heterozygous for the *ndl1-ref* mutation (Fig. 2 *D–F* and *SI Appendix*, Fig. S6). Sequencing of *ZmFTSH10* in these plants identified 4 different Cas9-induced frame-shift insertions and deletions (*SI Appendix*, Fig. S6), confirming that mutations in *ZmFTSH10* caused the aberrant tassel phenotype. We also generated transgenic plants containing a *pZmFTSH10*::*FTSH10*:*YFP* construct and crossed it to *ndl1-ref* homozygous mutants. Four independent events expressing the ZmFTSH10-YFP fusion protein were capable of fully complementing the *ndl1-ref* phenotype (Fig. 2*G* and *SI Appendix*, Fig. S7), further confirming that *NDL1* corresponds to *ZmFTSH10*/*GRMZM2G038401*.

Based on publicly available RNA-seq data and qRT-PCR in different tissues, *NDL1* is expressed ubiquitously in all tissues (*SI Appendix*, Fig. S8), and confocal analysis of *pZmFTSH10*::*FTSH10*:*YFP* transgenic lines showed that NDL1-YFP was present in all tissues examined, appearing as multiple punctate dots within each cell (Fig. 2*K* and *SI Appendix*, Fig. S8). Simultaneous imaging of NDL1-YFP with a mitochondrial marker in maize transgenic lines showed colocalization of the 2 signals, indicating that NDL1 was targeted to mitochondria as predicted (Fig. 2*L*).

FTSHs are ATP-dependent metalloproteases belonging to the AAA protein super family and ensure membrane protein quality control via proteolytic and chaperone-like activities (15). In eukaryotes, FTSHs are nuclear-encoded proteins targeted to chloroplasts and/or mitochondria. Mitochondrial FTSHs are grouped into the m-AAA and i-AAA classes, both localized in the inner membrane system: the m-AAA class has the active site facing the mitochondria matrix, whereas the i-AAA class exposes its catalytic sites to the inner membrane space. *Arabidopsis* contains 12 FTSH proteins, 4 of which are targeted to mitochondria via an N-terminal target peptide, including 2 m-AAA proteases, AtFTSH3 and AtFTSH10, and 2 i-AAA proteases, AtFTSH4 and AtFTSH11 (22, 23). The maize B73v3 reference genome contains 12 FTSH members. Neighbor-joining analysis placed NDL1 within the clade of m-AAA proteases that includes AtFTSH3 and AtFTSH10 and yeast YTA10 and YTA12 (*SI Appendix*, Fig. S9). Overall, NDL1 shares 74% and 71% identity and 82% and 78% similarity with AtFTSH3 and AtFTSH10, respectively. Two additional partially truncated genes, *LOC103629414* and *LOC109941663*, encoding proteins with ∼300 amino acids similar with the NDL1 N terminus, were also identified (*SI Appendix*, Fig. S10). However, both genes lacked sequence encoding all C-terminal domains, and they are likely nonfunctional. Therefore, NDL1 appears to be the only functional maize m-AAA protease.

To test whether the role of NDL1 in reproductive development was conserved, we analyzed *Arabidopsis Atftsh3* and *Atftsh10* mutants. We first obtained a T-DNA insertion line in *AtFTSH3* (SALK_037144) that knocked out *AtFTSH3* expression (*SI Appendix*, Fig. S11). Subsequently, we used CRISPR-Cas9 to edit *AtFTSH10* in the *ftsh3* insertion line background. A single T2 line, *CR-ftsh10*, carrying a 4-bp deletion in the coding region of *AtFTSH10*, was selected for further analysis (*SI Appendix*, Fig. S11). No specific inflorescence phenotype was observed in *Atftsh3*;*Atftsh10* double mutant relative to wild type plants, even when grown at elevated temperatures. However, double-mutant *Atftsh3*;*Atftsh10* plants showed a reduction in primary root length when compared with wild type, a result consistent with a recent report (23), and, similar to *ndl1*, the root phenotype was enhanced at higher temperatures (*SI Appendix*, Fig. S11). These results suggest that maize reproductive development may be more sensitive to the absence of ZmFTSH10 activity than *Arabidopsis*.

Like other eukaryotic FTSH proteins, NDL1 contains an N-terminal mitochondrial target peptide and several conserved domains (Fig. 2*C*). These include an N-terminal FTSH extracellular domain (Pfam) flanked by 2 transmembrane regions and

a middle region comprising an AAA+ domain containing Walker A and B motifs and an SRH motif, which are crucial for ATPase function. The C terminus contains a peptidase domain containing a Zn^{2+} binding HEXXH motif. The I541F mutation of the *ndl1-ref* mutant corresponds to a highly conserved residue located within the AAA+ lid domain (Pfam), which is important for ATPase activity (24) (*SI Appendix*, Fig. S10). We therefore measured the ATPase activity of recombinant NDL1 and *ndl1-ref* proteins and determined that the I541F mutation caused ~50% decrease in NDL1 ATPase activity independently of temperature (*SI Appendix*, Fig. S5), indicating that the temperature sensitivity of *ndl1* mutants was not specific to the *ndl1-ref* allele, but a common feature of mutants in this protein family (5, 23).

Alternative Respiration Complex and ROS-Related Genes Are Up-Regulated in *ndl1*. To better understand the molecular phenotype of *ndl1*, we performed RNA-seq on immature tassels and identified 1,199 up- and 831 down-regulated genes in *ndl1* mutants compared with wild type. In agreement with the role of plant m-AAA proteases in the stability and assembly of mitochondrial oxidative phosphorylation complexes, up-regulated genes in *ndl1* included many encoding mitochondrial-localized proteins such as those involved in mitochondria proficiency (i.e., *PROHIBITINS*; *PHBs*), as well as components of the electron transport chain (OXPHOS pathway) such as *AOX* (*ALTERNATIVE OXIDASE*), *type II NADPH dehydrogenases* (*NDBs*/*NDHs*), *COX17*/*COX19*, and *CYTC-1* (Fig. 3*A*) (25). *AOX* and *NDBs* are involved in alternative respiration pathways that serve as plant-specific bypasses of the electron transport chain and were among the highest up-regulated genes (*SI Appendix*, Table S1). Strong up-regulation was also observed in genes involved in oxidative stress and redox/detoxification such as *RESPIRATORY BURST OXYGEN* (*RBOHD*), *GLUTAREDOXINS* (*GRXs*), and several *GST*-encoding genes (Fig. 3*A* and *SI Appendix*, Table S1).

Arabidopsis homologs of these genes are implicated in mitochondrial retrograde signaling, which communicates suboptimal mitochondria status with the nucleus to restore cellular homeostasis (26, 27). *ndl1* tassels showed 26-fold up-regulation of the *AOX2* gene (*AOX1a* in *Arabidopsis*), which is known to counteract excess ROS caused by stress or mitochondrial defects in complex I (28, 29) (Fig. 3*A*). Only *AOX2*, but not other *AOX* members that act in different complexes (29), was up-regulated, indicating that *NDL1* may be specifically involved in complex I assembly (*SI Appendix*, Fig. S12). Furthermore, many genes homologous to other retrograde signaling marker genes (Fig. 3*A*) (30, 31) were significantly up-regulated, including small heat shock protein *ZmHSP23.5*, *UP-REGULATED BY OXIDATIVE STRESS* (*UPOX*) genes, and several *PHBs*, which physically interact with m-AAA proteases (32) (Fig. 3*A*). Comparison of transcriptional profiles of *Arabidopsis phb3* mutant roots (33)

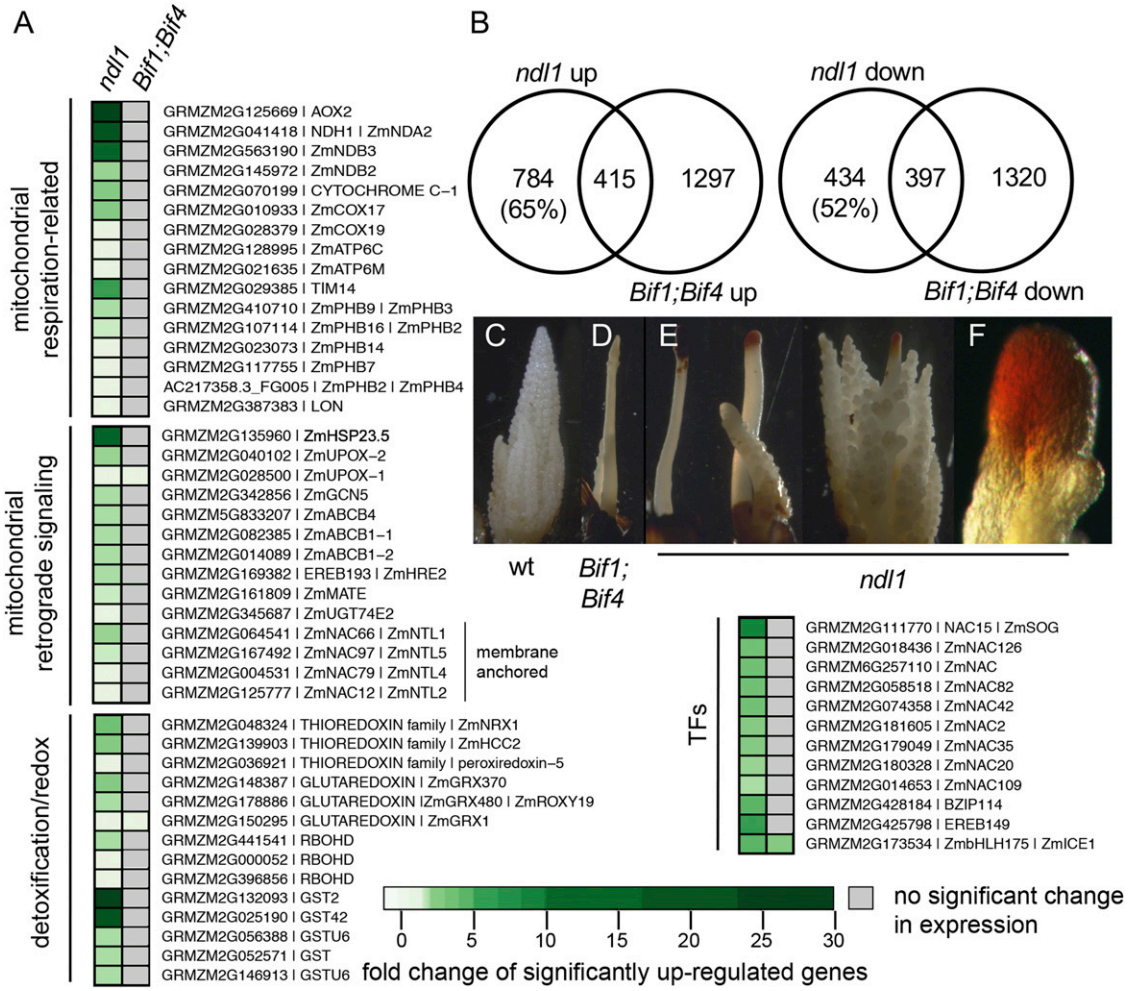

Fig. 3. *ndl1* inflorescences are stressed. (*A*) Genes significantly up-regulated in *ndl1* and *Bif1*;*Bif4* RNA-seq tassel datasets. Gray boxes indicate no significant expression difference observed relative to wild type (FDR < 0.05). (*B*) Overlap between differentially expressed genes (FDR < 0.05) in *ndl1* dataset and *Bif1*;*Bif4* dataset. (*C*–*F*) DAB staining of immature tassels to measure H_2O_2 accumulation. Strong DAB stain is observed only in IMs showing a very severe phenotype, but not in BMs where AMs are forming. Close-up view of IM in *F*.

and maize *ndl1* tassels showed over 100 orthologous genes that were up-regulated in both mutants (*SI Appendix*, Table S1 and Dataset S1), indicating that compromised NDL1 function results in a similar transcriptional response to that seen in *Arabidopsis* under various mitochondrial perturbations, and suggesting conserved retrograde signaling components between these 2 distantly related species. Additional genes that may be involved in mitochondrial stress response include *ZmNAC15*, a homolog of an *Arabidopsis* DNA damage response regulator (34), and *ZmEREB149*, a close homolog of *AtERF114* that mediates ROS signaling (33) (Fig. 3*A* and *SI Appendix*, Table S1).

To understand whether the transcriptional changes observed in *ndl1* tassels were a consequence of the severe inflorescence phenotype, we also performed RNA-seq on immature tassels of the *Bif1*;*Bif4* auxin signaling mutant, which displays a similar phenotype to *ndl1* (14), and then carried out comparative transcriptomic analysis. Over 65% (784 of 1,199) of up-regulated genes and 52% (434 of 8,31) of down-regulated genes in the *ndl1* dataset were not found in *Bif1*;*Bif4*, reflecting largely distinct molecular signatures for each mutant (Fig. 3*B*). Genes specifically up-regulated in *ndl1* but not *Bif1*;*Bif4* included all members of the OXPHOS pathway, certain *GSTs*, *NACs*, and *EREB149* (Fig. 3*A*). GO analysis of genes differentially expressed in both *ndl1* and *Bif1*;*Bif4*, *ndl1*-only, or *Bif1*;*Bif4*-only mutants showed enrichment for the terms "response to chemical, biotic and abiotic stimulus" and "response to stress" for most subsets (*SI Appendix*, Fig. S12). Down-regulated genes found in both the shared and *Bif1*;*Bif4* datasets included those involved in early reproductive development such as *BA1* (16), likely absent due to lack of AMs in both mutants (*SI Appendix*, Fig. S12). On the contrary, down-regulated genes found only in *Bif1*;*Bif4* showed strong enrichment for "chromatin assembly" and "protein folding" supporting a link between auxin signaling and changes in chromatin state (35) (*SI Appendix*, Fig. S12).

Since mitochondria are a main source of ROS, and OXPHOS complex defects increase ROS production (36), we performed DAB staining to examine H_2O_2 levels in immature tassels (Fig. 3 *C*–*F*). No staining was observed in wild type or *Bif1*;*Bif4* tassels (Fig. 3 *C* and *D*), but strong accumulation was detected at the tip of *ndl1* IMs displaying a strong barren phenotype but not in those with a less severe phenotype (Fig. 3*E* and *SI Appendix*, Fig. S13). DAB staining was observed only in the IM of the main spike and not in the middle, base, or in secondary branches, suggesting that the up-regulation of *AOX2* or scavenging enzymes (28) may quickly restore the redox status in these organs. These results are consistent with the hypothesis that NDL1 functions in maintaining OXPHOS complex activity.

***ndl1* Alters Endogenous Auxin Levels and Responses.** Given the role of auxin in the formation of lateral primordia and the synergistic interaction between *ndl1* and several auxin mutants, *NDL1* may regulate inflorescence development via cross-talk with auxin-related pathways. We therefore examined differentially expressed genes involved in auxin signaling, transport, and homeostasis in *ndl1* and *Bif1*;*Bif4* RNA-seq datasets, and observed that many genes including *PINs*, *ARFs*, *AUX/IAAs*, and *GH3s* were differentially expressed in both mutants. In general, genes within this subset of auxin-related genes showed similar transcriptional responses. For example, both mutants showed significant up-regulation of the auxin transporter gene *ZmPIN10* as well as mis-regulation of several *GH3* genes involved in auxin inactivation, indicating that auxin transport and homeostasis are similarly perturbed. On the contrary, several *Aux/IAA* genes were differentially expressed only in one mutant but not the other, suggesting that *Aux/IAAs* may function in specific contexts (*SI Appendix*, Fig. S13).

The strong genetic interactions observed with *Bif1*, which encodes a stabilized AUX/IAA protein insensitive to auxin-induced degradation (14), and with *spi1*, an auxin biosynthetic mutant (*SI Appendix*, Fig. S4), suggested that, in *ndl1* IMs, the levels of free auxin may be decreased and thus cause early defects in organogenesis. To test this hypothesis, we crossed *ndl1* to DII-VENUS, a marker line based on the degron domain of AUX/IAA proteins, whose degradation is controlled by auxin levels in cells (37, 38). In wild type tassels, low expression of DII-VENUS was detected in the IM, indicating relatively high concentration of endogenous auxin. In *ndl1* tassels with a severe phenotype, however, the DII-VENUS signal was stronger and uniformly distributed, indicating lower levels of auxin in *ndl1* IMs and in particular in the PZ (Fig. 4 *A* and *B* and *SI Appendix*, Fig. S13). This was not observed in *ndl1* tassels with a mild phenotype that resembled wild type DII-VENUS expression (*SI Appendix*, Fig. S13). We also investigated the response of *ndl1* roots to applications of 2,4D, a synthetic auxin analog, and measured the primary root length of treated and untreated wild type and *ndl1* mutants. 2,4D applications caused a significant reduction in primary root length and a proliferation of lateral roots in wild type as expected (39), while *ndl1* roots were less sensitive to the treatments (Fig. 4 *C* and *D*). These findings indicate that *ndl1* is partially buffered from exogenous auxin applications, suggesting that more auxin is needed to achieve a similar response to wild type roots and that fully functional mitochondria are necessary for a normal auxin response.

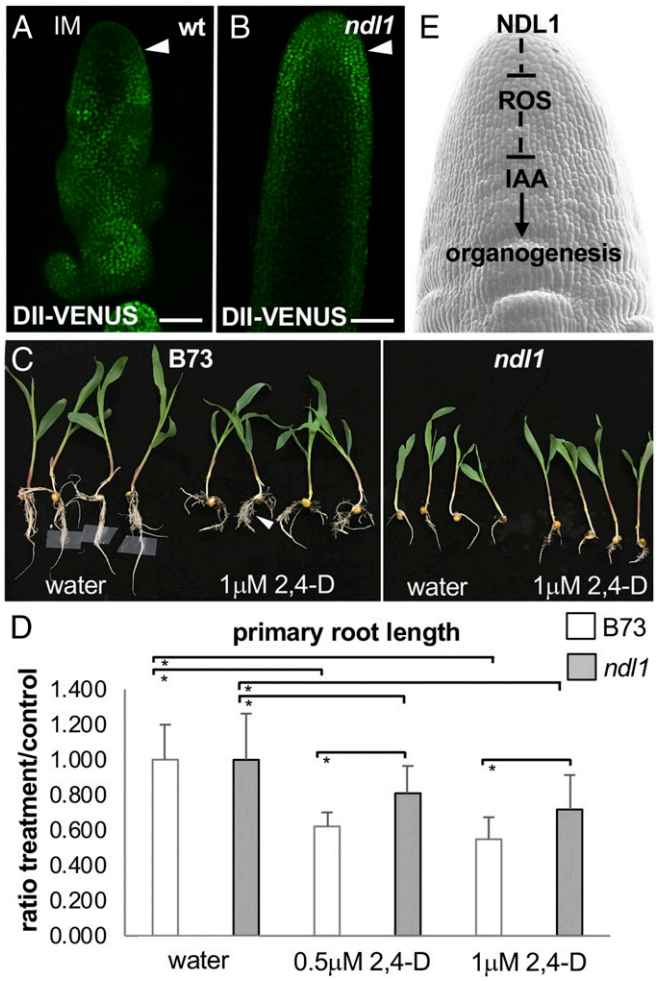

Fig. 4. Auxin-related defects in *ndl1* mutants. (*A* and *B*) Maximum projection of DII-VENUS signals in wild type (*A*) and *ndl1* mutant (*B*) immature tassels. IM, inflorescence meristem. Arrowheads point to the PZ where high DII-VENUS signal is observed in *ndl1* but not in wild type. (Scale bars, 100 μm.) (*C* and *D*) *ndl1* roots are less sensitive to exogenous 2,4D applications ($n \geq 34$ per treatment; data from at least 2 biological replicates; error bars represent SD; $^*P < 0.0001$, Student's *t* test). (*E*) Schematic model of NDL1 function in organogenesis.

Discussion

Given their role in providing energy to cells and sensing environmental stresses, mitochondria are essential for plant growth (25). How mitochondrial status is integrated with developmental programs such as those controlled by auxin, however, remains unclear. Here we demonstrate that NDL1, a mitochondria-localized m-AAA protease, is necessary for thermotolerant growth of maize. Mitochondrial FTSH proteins are highly conserved across taxa at the sequence and functional levels, form oligomeric complexes, and, together with PHBs, are required for proper assembly and maintenance of mitochondrial oxidative phosphorylation complexes (15, 40). In *ndl1* mutants, ROS accumulate to high levels in IMs, mitochondria switch to the alternative oxidase pathway, and meristem defects lead to altered inflorescence architecture. These phenotypes resemble those reported in related *Arabidopsis* mutants such as *ftsh4* and the type-I prohibitin *phb3*, which show elevated ROS and *AOX* levels as well as SAM defects and increased shoot branching (5, 7, 33, 41). It is therefore surprising that *Arabidopsis ftsh3;ftsh10* mutants did not show an obvious and specific reproductive phenotype but rather displayed only root growth defects (here and in ref. 23). This difference could reflect the fact that high-temperature field conditions are sufficient to trigger the *ndl1* phenotype, while the relatively cool standard growth conditions of *Arabidopsis* are not. Indeed, *ndl1* mutants grown at mild temperatures showed no phenotype. Only when grown at constant high temperatures in a controlled environment were *ndl1* mutants also impaired in vegetative development, suggesting that the apparent inflorescence-specific phenotype of *ndl1* mutants is due to the seasonal maize growth (i.e., germinating in mild temperatures and transitioning to reproductive development in warmer temperatures).

The effect on maize organogenesis caused by the *ndl1* mitochondria-related defects resembled that seen in auxin-related mutants, and our analysis showed a synergistic interaction at the genetic level among mutants, a decrease in endogenous auxin levels and auxin transport in *ndl1* inflorescences, and attenuated response to exogenous auxin applications in roots. Transcriptional analysis of *ndl1* tassels showed the mis-regulation of many auxin-related genes, similar to those observed in the maize *Bif1*;*Bif4* auxin signaling mutant (14). However, *ndl1* displayed several unique phenotypes such as elevated accumulation of H_2O_2 in IMs and a large number of strongly up-regulated ROS-scavenger and redox-related genes, such as those belonging to the *PEROXIDASE*, *GST*, and the *THIOREDOXIN* families (Fig. 3*A* and *SI Appendix*, Fig. S12). ROS contribute to plant development and stress responses and may directly influence auxin homeostasis, transport, and signaling (10, 26), i.e., H_2O_2 was proposed to mediate auxin oxidative degradation via peroxidase activities (7, 42). Such a scenario agrees with lower auxin levels in *ndl1* IMs with high ROS. However, we also observed several genes involved in auxin conjugation, such as *ZmGH3.2* and *ZmGH3.8* and *UDP-glucosyl transferase* genes (43), that were up-regulated in *ndl1*. One of the latter genes, *UGT74E2*, is often up-regulated in mitochondrial stress responses (44). Furthermore, high temperatures directly influence auxin levels (45), highlighting the inherent complexity of these interactions. We propose that *NDL1* is required for maintaining the redox status of meristems to sustain maize growth at high temperatures (Fig. 4*E*). When impaired, stress signals unbalance auxin regulation at the PZ of IMs, which results in defective organogenesis. While heat stress enhances the *ndl1* phenotype, it is likely that other stresses also influence it. Indeed, RNA-seq of *ndl1* tassels showed up-regulation of many genes whose *Arabidopsis* homologs have been associated with mitochondrial stresses, dysfunction, and retrograde signaling (46), uncovering many genes likely to regulate maize growth under duress. Understanding how *NDL1* and other mitochondrial stress-related genes function is essential to devise strategies for enhancing maize yield in suboptimal environments and harsher climates.

Materials and Methods

The *ndl1* reference (*ndl1-ref*) allele was generated by EMS mutagenesis in the OH43 background by Gerald Neuffer and obtained from the Maize Genetics Cooperation Stock Center (stock 04HI-A632XOH43GN-173; original M2 population). Complete details regarding plant materials, experimental methods, and data analyses are provided in the *SI Appendix*.

ACKNOWLEDGMENTS. The authors thank Dr. Gerald Neuffer for generating the *ndl1-ref* allele, the Maize Genetics Cooperation Stock Center for seeds, Renyta Moses and Gabriel Koslow for help with genotyping, Paula McSteen and the University of Missouri Columbia Plant Transformation Core Facility for transformation, Robert Schmitz and the Georgia University Genetic Department for RNA-seq sequencing, Yaping Feng for assistance with BSA RNA-seq, and Carolyn Rasmussen for DII-VENUS seeds and comments on the manuscript. Q.L. was supported by the China Scholarship Council and by the Waksman Charles and Johanna Busch Fellowship. This research was supported by grants from the National Science Foundation (IOS 1546873 and 1456950 to A.G.).

1. A. Pfeiffer, C. Wenzl, J. U. Lohmann, Beyond flexibility: Controlling stem cells in an ever changing environment. *Curr. Opin. Plant Biol.* **35**, 117–123 (2017).
2. B. Shi, T. Vernoux, Patterning at the shoot apical meristem and phyllotaxis. *Curr. Top. Dev. Biol.* **131**, 81–107 (2019).
3. J. Zeng, Z. Dong, H. Wu, Z. Tian, Z. Zhao, Redox regulation of plant stem cell fate. *EMBO J.* **36**, 2844–2855 (2017).
4. T. Bashandy *et al.*, Interplay between the NADP-linked thioredoxin and glutathione systems in Arabidopsis auxin signaling. *Plant Cell* **22**, 376–391 (2010).
5. A. Dolzblasz *et al.*, The mitochondrial protease AtFTSH4 safeguards Arabidopsis shoot apical meristem function. *Sci. Rep.* **6**, 28315 (2016).
6. F. Yang *et al.*, A maize glutaredoxin gene, abphyl2, regulates shoot meristem size and phyllotaxy. *Plant Cell* **27**, 121–131 (2015).
7. S. Zhang *et al.*, Perturbation of auxin homeostasis caused by mitochondrial FtSH4 gene-mediated peroxidase accumulation regulates arabidopsis architecture. *Mol. Plant* **7**, 856–873 (2014).
8. J. Knuesting *et al.*, Arabidopsis glutaredoxin S17 and its partner, the nuclear factor Y subunit C11/negative cofactor 2α, contribute to maintenance of the shoot apical meristem under long-day photoperiod. *Plant Physiol.* **167**, 1643–1658 (2015).
9. L. Hong *et al.*, Variable cell growth yields reproducible organ development through spatiotemporal averaging. *Dev. Cell* **38**, 15–32 (2016).
10. V. B. Tognetti, A. Bielach, M. Hrtyan, Redox regulation at the site of primary growth: Auxin, cytokinin and ROS crosstalk. *Plant Cell Environ.* **40**, 2586–2605 (2017).
11. J. H. Schippers, C. H. Foyer, J. T. van Dongen, Redox regulation in shoot growth, SAM maintenance and flowering. *Curr. Opin. Plant Biol.* **29**, 121–128 (2016).
12. A. Gallavotti *et al.*, Sparse inflorescence1 encodes a monocot-specific YUCCA-like gene required for vegetative and reproductive development in maize. *Proc. Natl. Acad. Sci. U.S.A.* **105**, 15196–15201 (2008).
13. Y. Zhao, Auxin biosynthesis. *Arabidopsis Book* **12**, e0173 (2014).
14. M. Galli *et al.*, Auxin signaling modules regulate maize inflorescence architecture. *Proc. Natl. Acad. Sci. U.S.A.* **112**, 13372–13377 (2015).
15. T. Ogura, A. J. Wilkinson, AAA+ superfamily ATPases: Common structure–Diverse function. *Genes Cells* **6**, 575–597 (2001).
16. A. Gallavotti *et al.*, The role of barren stalk1 in the architecture of maize. *Nature* **432**, 630–635 (2004).
17. P. McSteen *et al.*, Barren inflorescence2 Encodes a co-ortholog of the PINOID serine/threonine kinase and is required for organogenesis during inflorescence and vegetative development in maize. *Plant Physiol.* **144**, 1000–1011 (2007).
18. A. Gallavotti, Y. Yang, R. J. Schmidt, D. Jackson, The Relationship between auxin transport and maize branching. *Plant Physiol.* **147**, 1913–1923 (2008).
19. K. A. Phillips *et al.*, Vanishing tassel2 encodes a grass-specific tryptophan aminotransferase required for vegetative and reproductive development in maize. *Plant Cell* **23**, 550–566 (2011).
20. S. Liu, C. T. Yeh, H. M. Tang, D. Nettleton, P. S. Schnable, Gene mapping via bulked segregant RNA-Seq (BSR-Seq). *PLoS One* **7**, e36406 (2012).
21. R. Bukowski *et al.*, Construction of the third-generation Zea mays haplotype map. *Gigascience* **7**, 1–12 (2018).
22. A. Urantowka, C. Knorpp, T. Olczak, M. Kolodziejczak, H. Janska, Plant mitochondria contain at least two i-AAA-like complexes. *Plant Mol. Biol.* **59**, 239–252 (2005).
23. M. Kolodziejczak, R. Skibior-Blaszczyk, H. Janska, m-AAA complexes are not crucial for the survival of arabidopsis under optimal growth conditions despite their importance for mitochondrial translation. *Plant Cell Physiol.* **59**, 1006–1016 (2018).
24. J. M. Miller, E. J. Enemark, Fundamental characteristics of AAA+ protein family structure and function. *Archaea* **2016**, 9294307 (2016).
25. A. H. Millar, J. Whelan, K. L. Soole, D. A. Day, Organization and regulation of mitochondrial respiration in plants. *Annu. Rev. Plant Biol.* **62**, 79–104 (2011).
26. P. I. Kerchev *et al.*, Mitochondrial perturbation negatively affects auxin signaling. *Mol. Plant* **7**, 1138–1150 (2014).
27. J. D. Woodson, J. Chory, Coordination of gene expression between organellar and nuclear genomes. *Nat. Rev. Genet.* **9**, 383–395 (2008).

28. G. C. Vanlerberghe, Alternative oxidase: A mitochondrial respiratory pathway to maintain metabolic and signaling homeostasis during abiotic and biotic stress in plants. *Int. J. Mol. Sci.* **14**, 6805–6847 (2013).
29. O. V. Karpova, E. V. Kuzmin, T. E. Elthon, K. J. Newton, Differential expression of alternative oxidase genes in maize mitochondrial mutants. *Plant Cell* **14**, 3271–3284 (2002).
30. I. De Clercq *et al*., The membrane-bound NAC transcription factor ANAC013 functions in mitochondrial retrograde regulation of the oxidative stress response in Arabidopsis. *Plant Cell* **25**, 3472–3490 (2013).
31. O. Van Aken *et al*., Defining the mitochondrial stress response in Arabidopsis thaliana. *Mol. Plant* **2**, 1310–1324 (2009).
32. G. Steglich, W. Neupert, T. Langer, Prohibitins regulate membrane protein degradation by the m-AAA protease in mitochondria. *Mol. Cell. Biol.* **19**, 3435–3442 (1999).
33. X. Kong *et al*., PHB3 maintains root stem cell niche identity through ROS-Responsive AP2/ERF transcription factors in Arabidopsis. *Cell Rep.* **22**, 1350–1363 (2018).
34. C. Bourbousse, N. Vegesna, J. A. Law, SOG1 activator and MYB3R repressors regulate a complex DNA damage network in *Arabidopsis*. *Proc. Natl. Acad. Sci. U.S.A.* **115**, E12453–E12462 (2018).
35. D. Weijers, D. Wagner, Transcriptional responses to the auxin hormone. *Annu. Rev. Plant Biol.* **67**, 539–574 (2016).
36. I. G. Kirkinezos, C. T. Moraes, Reactive oxygen species and mitochondrial diseases. *Semin. Cell Dev. Biol.* **12**, 449–457 (2001).
37. R. Mir *et al*., A DII domain-based auxin reporter uncovers low auxin signaling during telophase and early G1. *Plant Physiol.* **173**, 863–871 (2017).
38. G. Brunoud *et al*., A novel sensor to map auxin response and distribution at high spatio-temporal resolution. *Nature* **482**, 103–106 (2012).
39. M. V. Alarcón, J. Salguero, P. G. Lloret, Auxin modulated initiation of lateral roots is linked to pericycle cell length in maize. *Front. Plant Sci.* **10**, 11 (2019).
40. J. Piechota, M. Kolodziejczak, I. Juszczak, W. Sakamoto, H. Janska, Identification and characterization of high molecular weight complexes formed by matrix AAA proteases and prohibitins in mitochondria of Arabidopsis thaliana. *J. Biol. Chem.* **285**, 12512–12521 (2010).
41. O. Van Aken *et al*., Mitochondrial type-I prohibitins of Arabidopsis thaliana are required for supporting proficient meristem development. *Plant J.* **52**, 850–864 (2007).
42. T. Kawano, Roles of the reactive oxygen species-generating peroxidase reactions in plant defense and growth induction. *Plant Cell Rep.* **21**, 829–837 (2003).
43. K. Tanaka *et al*., UGT74D1 catalyzes the glucosylation of 2-oxindole-3-acetic acid in the auxin metabolic pathway in Arabidopsis. *Plant Cell Physiol.* **55**, 218–228 (2014).
44. V. B. Tognetti *et al*., Perturbation of indole-3-butyric acid homeostasis by the UDP-glucosyltransferase UGT74E2 modulates Arabidopsis architecture and water stress tolerance. *Plant Cell* **22**, 2660–2679 (2010).
45. K. A. Franklin *et al*., Phytochrome-interacting factor 4 (PIF4) regulates auxin biosynthesis at high temperature. *Proc. Natl. Acad. Sci. U.S.A.* **108**, 20231–20235 (2011).
46. Y. Wang *et al*., Stress responsive mitochondrial proteins in Arabidopsis thaliana. *Free Radic. Biol. Med.* **122**, 28–39 (2018).